NLC Positron Production Target

O. E. Krivosheev, N. V. Mokhov and S. I. Striganov[+]

Fermi National Accelerator Laboratory

P.O. Box 500, Batavia, Illinois 60510

[+] *Institute for High Energy Physics, Protvino, 142284, Russia*

April 19, 1996

Abstract

The NLC positron production target is optimized with respect to positron yield, target integrity, cooling and shielding. Copper is proposed as a possible optimal choice.

1 Introduction

The proposed Next Linear Collider (NLC) is a e^+e^- linear collider with the c. m. energy 500 GeV in phase I and 1 TeV in phase II [1]. One of the essential NLC components is a positron source for producing a low energy positron beam to be captured and accelerated. The positron production target design should take into account and properly balance the positron yield per initial electron, target integrity, shielding and thermal problems. In this study the EGS4 [3], GEANT3 [4] and MARS13 [5] Monte Carlo codes are used for electromagnetic shower simulations and the ANSYS code [6] for thermal and stress analyses. The positron yield and target behaviour are studied for a few target materials and configurations both for NLC-I and NLC-II beam parameters.

2 Design and Calculation Parameters

The relevant parameters of the NLC positron source for both the 0.5 TeV and the 1 TeV machines are presented in Table 1 [1]. For both phases, pulse duration is 126 ns and bunch spacing is 1.4 ns.

Table 1: Positron source parameters.

Parameter	NLC-I	NLC-II
Energy E_{e^-}, GeV	3.11	6.22
No. of e^- per bunch	1.50×10^{10}	1.50×10^{10}
No. of bunches per pulse	90	90
No. of e^- per pulse	1.35×10^{12}	1.35×10^{12}
Repetition rate, Hz	180	120
Beam power, kW	121	161
Beam RMS, mm	1.2	1.6
Bunch intensity at IP	0.84×10^{10}	1.24×10^{10}

Positrons generated in the target are captured into a flux concentrator with the minimum radius of the internal cone R_{col}=4.5 mm in the energy range 2 to 22 MeV. The positron bunch accelerated in the linac goes finally to the collider. According to [1, 2], one can get about 2.1×10^{10} and 3.1×10^{10} positrons per bunch from the disc tungsten target for NLC-I and NLC-II, respectively, that is a factor of 2.5 higher than the bunch intensity required at the interaction point (IP) (see Table 1).

It is assumed that the incident on the target electron beam has a Gaussian spatial distribution with $\sigma_x = \sigma_y = 1.2\ (1.6)$ mm, a Gaussian energy distribution with $\sigma_E = 0.001 \times E_{e^-}$ and a Gaussian angular distribution with $\sigma_\theta = 0.5$ mrad. Calculations of the positron yield and energy deposition in the targets have been performed for

the above electron beam parameters. All the three codes, EGS4, GEANT3 and MARS, predict both yield and energy deposition in a remarkable agreement with each other and with results of [1].

Tungsten gives a maximum positron yield, but it is fragile and has low specific heat and thermal conductivity, that leads to severe mechanical and cooling problems. A mitigation is possible with tungsten alloys. In the baseline design, the target is assumed to be made of a $W_{75}R_{25}$ tungsten-rhenium alloy with a thickness of 4 radiation length (L_R). Experience at the Fermilab Pbar Source has shown an excellent behaviour of copper targets under extreme irradiation conditions (see below). Its relatively low Z can result in somewhat decreased positron yield, but copper is far superior from the mechanical and thermal standpoints.

Both $W_{75}R_{25}$ and copper targets of various thicknesses are studied here. Three target configurations are considered: a disc of R=100 cm radius, a cylinder of R=4 and 6 mm radius and a cone with the upstream radius R_1=5 mm and the downstream one R_2=3 mm. The studies show that the maximum positron yield in the energy bin of 2 to 22 MeV is from the $5L_R$ tungsten ($W_{75}R_{25}$) and $4L_R$ copper targets. The energy deposition density at the downstream end of a $5L_R$ tungsten target becomes too high, so, as in [1], we have accepted for $W_{75}R_{25}$ also the $4L_R$ thickness.

3 Positron Yield

Figure 1 shows the calculated positron yield per incident electron for a disc tungsten target $4L_R$ thick for several collection radii R_{col} for the NLC-I and NLC-II, respectively, as a function of the positron energy. Being integrated in the energy interval 2 to 22 MeV, results are rather close to those of [1]. Possible techniques to increase the yield were proposed in [7]. To study those, the three target geometries and different collection radii are explored in a wider energy region. Positron yields from the copper targets of three configurations are presented in Figure 2 through Figure 5 as a ratio to those from the disc tungsten target. Table 2 gives the ratios for the disc, cylinder and cone copper targets for two collection radii for NLC-I and NLC-II.

Table 2: Ratio of the positron yield in the 2 to 22 MeV energy interval from the copper targets to that from the disc tungsten target.

Target	Disc	Cyl-4	Cyl-6	Cone
	R_{col} = 5 mm			
NLC-I	0.55	0.53	0.54	0.54
NLC-II	0.57	0.53	0.57	0.54
	R_{col} = 10 mm			
NLC-I	0.66	0.71	0.69	0.71
NLC-II	0.68	0.71	0.71	0.72

Positron yield from copper is about 55 to 72% of that from tungsten in the energy interval 2 to 22 MeV. As expected for given parameters, the yields from the copper targets are lower compared to those from the tungsten. At the same time, the yield from a cone copper target with R_{col}=10 mm is rather close to the design goal. For a fixed electron beam intensity, the main gain with copper can come from the thermal, mechanical and shielding considerations.

4 Thermal and Structural Analyses

Energy deposition density in tungsten and copper targets 6 mm in radius is shown in Figures 6 and 7, respectively. One can see that the copper target has less energy deposited per unit volume. On the other hand, integral energy depositions are rather close to each other for the same target lengths as shown in Table 3.

Table 3: Fraction of the beam energy (%) deposited in tungsten and copper disc targets of different lengths L (in units of the radiation length L_R). Last column shows the peak energy deposition density ϵ_{max} for the $4L_R$ thick target.

		L=2	4	6	8	ϵ_{max} (J/g)
NLC-I	W	4.0	20.6	43.7	64.0	67
NLC-I	Cu	6.7	29.1	55.2	74.5	29
NLC-II	W	2.5	15.0	36.2	56.9	73
NLC-II	Cu	4.1	21.7	46.5	67.7	35

High energy deposition in targets cause high temperature and pressure at the beam axis, and this disturbance propagates outwards as a shock wave which can result in crack formation and fracture [8]. The CERN Antiproton Accumulator target sustained a maximum energy deposition of approximately 185 Joules per gram for tungsten [9]. Rhenium and tungsten(75%)–rhenium(25%) alloy demonstrated better behaviour [1, 9, 10]. Both detailed calculations [8] and experience [10, 11] have shown that copper sustains much higher energy deposition density, in excess of 500 J/g. Observed with a 120 GeV proton beam (1.6×10^{12} protons per 1.6 μsec pulse every 2.4 sec) peak energy deposition in copper is 512 J/g with no sign of damage over long periods of repeatetative irradiation, with no structural changes up to the melting point limit of 613 J/g [12]. It is explained by the fact that only about 5% of the total energy deposition density in copper is converted into mechanical energy resulting in the pressure of about a few GPa (compare to Young's modulus for copper of 123.5 GPa) [8]. Currently the Pbar Source target at Fermilab is made of nickel with no target depletion effects observed for the peak energy deposition of 615 J/g [10]. A preliminary ANSYS stress analysis in a copper target (R=6 mm)

for the NLC-II beam parameters gives an equivalent stress of about 1 GPa immediately after the first bunch and the maximum displacement of about 0.014 mm at the downstream end of the target.

Calculated peak energy deposition densities in the tungsten alloy targets are rather high. For this reason, special mitigating measures are proposed in [1] to prevent target destruction: a spoiler to increase the initial beam spot size and a target rotation with a high speed. Nevertheless, it is unlikely that the tungsten-based targets can handle a few times higher electron beam intensity compared to that of Table 1.

Contrary, the calculated above peak energy density in copper is about 7% of the corresponding melting point limit (a real limit for copper as per [8, 10, 11, 12]). The use of copper can drastically simplify the target operation: no spoilers, no target rotations. With the current proposal, the tungsten target provides about 40% higher positron yield, with only a factor of two reserve for further increasing of the production rate. At the same time, copper has at least a factor of fifteen margin, which allows an increase of the positron yield just by using more intense electron beam. One can get up to 3×10^{11} positrons per bunch with a copper target and even more with the nickel target with an appropriate cooling system provided.

In a thermal analysis with ANSYS the effective cooling system with ΔT=0 at the target outer radius was assumed. Figure 8 shows a two-dimensional maximum temperature distribution in the copper target 0.4 sec after the beginning of the irradiation. Figure 9 shows the time dependence of maximum temperature in the copper target with a steady-state regime reached after about 0.3 sec. One can see that with a good cooling system the maximum temperature in the target is $\approx 450^{\circ}$C, that allows one to stay with a stationary device.

5 Shielding

A copper target has another advantage, lower neutron yield, which reduces the required shielding. Calculated with the MARS code, hadron (E$>$ 14 MeV) and low-energy neutron (E$<$ 14 MeV) fluxes around tungsten and copper targets are presented in Table 4. The neutron yield is almost 6 times lower for the copper target, that results in a more compact target zone shielding. Estimated residual dose rate for the copper target is lower compared to the tungsten one.

Table 4: Particle fluxes around the tungsten and copper targets (4 L_R long and 6 mm radius) irradiated with 6.22 GeV electron beam at 120 Hz rate.

Target	Φ_n (cm^{-2}s^{-1})	Φ_h (cm^{-2}s^{-1})
W	$6.25\cdot10^{12}$	$4.72\cdot10^{11}$
Cu	$1.04\cdot10^{12}$	$4.39\cdot10^{11}$

6 Conclusions

Copper is suggested as a possible material for the positron production target with the yield close to the tungsten one. In contrast to tungsten, copper is farther from the shock-wave limit and has much better thermal properties. A copper target can be designed as a stationary unrotated cylinder with intensive cooling. With a copper target it is possible to increase further positron yield using a more intense e^- beam. Hadron and low-energy neutron yield is lower for the copper target in comparison with the tungsten one, reducing the volume of the required shielding.

7 Acknowledgments

The authors wish to thank Mike Foley, Bruce Hoffman and Mark Reichanadter for their help with the ANSYS thermal calculations, Igor Novitski for the target stress analysis and Jim Holt and Artem Kulikov for useful discussions.

References

[1] "NLC ZDR Report, March Workbook" (1995). Current version is in preparation.

[2] H. Tang, private communication, April 1996.

[3] W. Nelson, H. Hirayama and D. Rogers, "The EGS-4 Code System", SLAC Report–265 (1985).

[4] "GEANT, Detector Description and Simulation Tool", CERN, Geneva (1994).

[5] N. V. Mokhov, "The MARS code system Users Guide, version 13(95)", Fermilab–FN–628 (1995).

[6] "ANSYS User's Manual", Vol. I and II, SASI Publications (1994).

[7] R. Donahue and W. Nelson, "Alternative Positron Target Design for Electron-Positron Colliders", SLAC–Pub–5702 (1991).

[8] Z. Tang and K. Anderson, "Shock Waves in P-bar Target", Fermilab–TM–1763 (1991).

[9] Proc. of "High Intensity Targeting Workshop", Fermilab, April 28-30 (1980).

[10] S. O'Day, F. Bieniosek, and K. Anderson, "New Target Results from the FNAL Antiproton Source", *Proc. of the 1993 IEEE Particle Accelerator Conference*, 3096 (1993).

[11] F. M. Bieniosek, “Effect of Melting on Target Performance”, Fermilab Pbar Note–512 (1991).

[12] S. O’Day, private communication, April 1996.

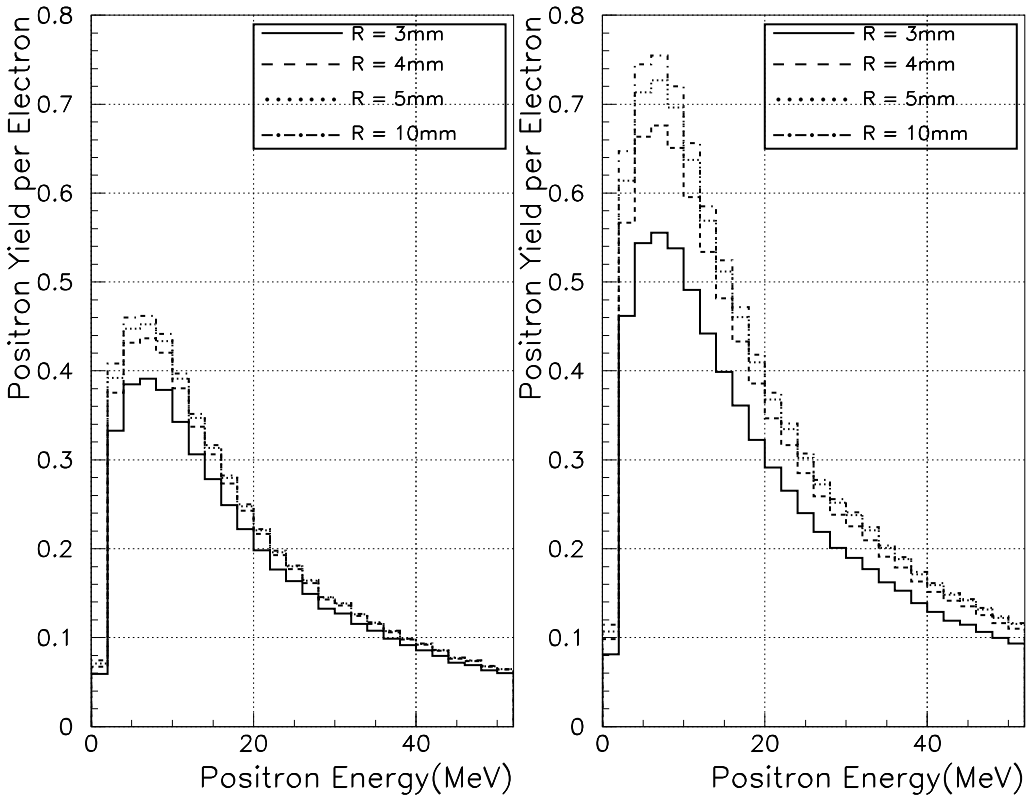

Figure 1: Positron yield per ΔE=2 MeV per one electron for the disc tungsten target. a) E_{e^-}=3.11 GeV, σ_x=σ_y= 1.2 mm (left); b) E_{e^-}=6.22 GeV, σ_x=σ_y= 1.6 mm (right).

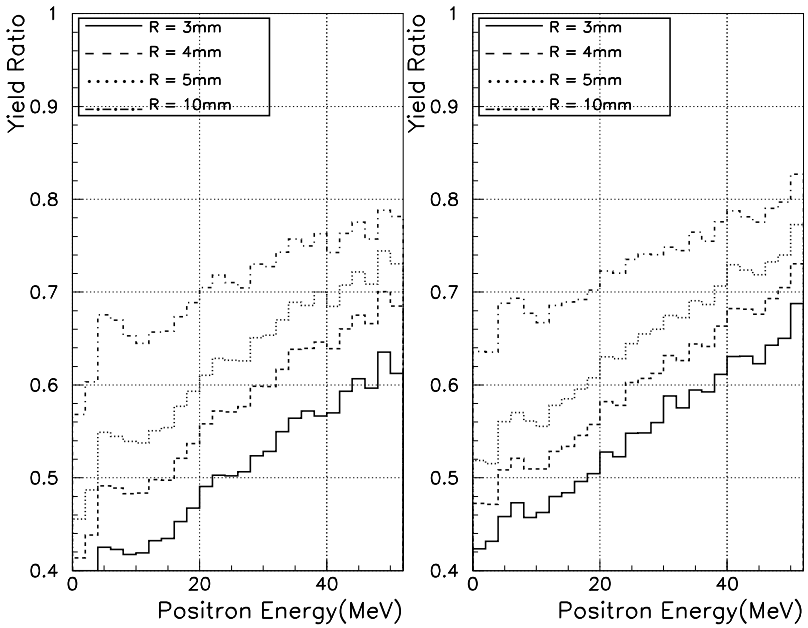

Figure 2: Ratio of positron yield per ΔE=2 MeV from the disc copper target to that from the tungsten one. a) E_{e^-}=3.11 GeV, σ_x=σ_y= 1.2 mm (left); b) E_{e^-}=6.22 GeV, σ_x=σ_y= 1.6 mm (right).

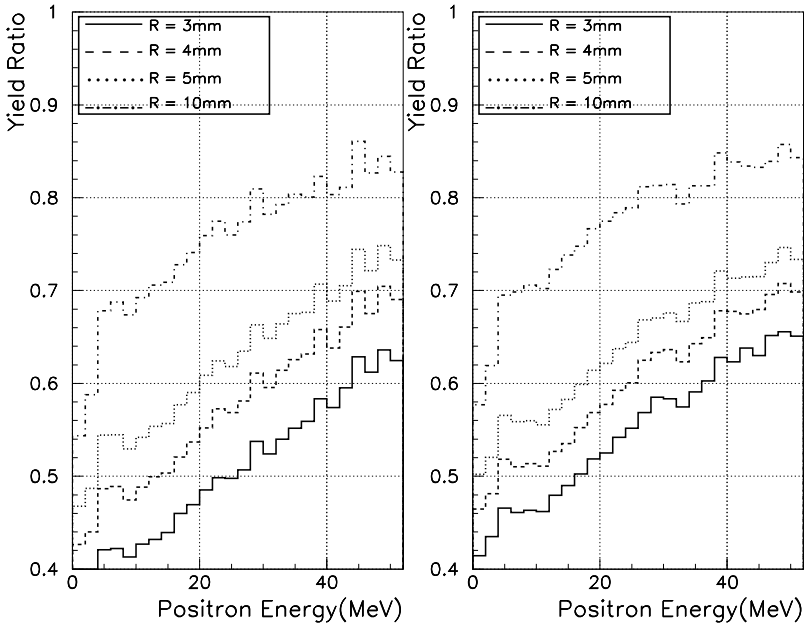

Figure 3: Ratio of positron yield per ΔE=2 MeV from the cylinder copper target (R=6 mm) to that from the tungsten disc. a) E_{e^-}=3.11 GeV, σ_x=σ_y= 1.2 mm (left); b) E_{e^-}=6.22 GeV, σ_x=σ_y= 1.6 mm (right).

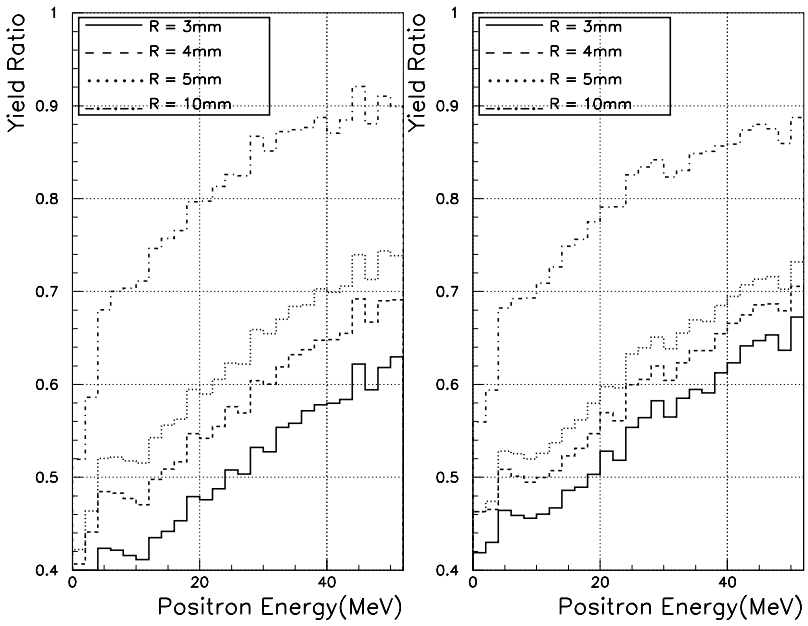

Figure 4: Ratio of positron yield per ΔE=2 MeV from the cylinder copper target (R=4 mm) to that from the tungsten disc. a) E_{e^-}=3.11 GeV, σ_x=σ_y= 1.2 mm (left); b) E_{e^-}=6.22 GeV, σ_x=σ_y= 1.6 mm (right).

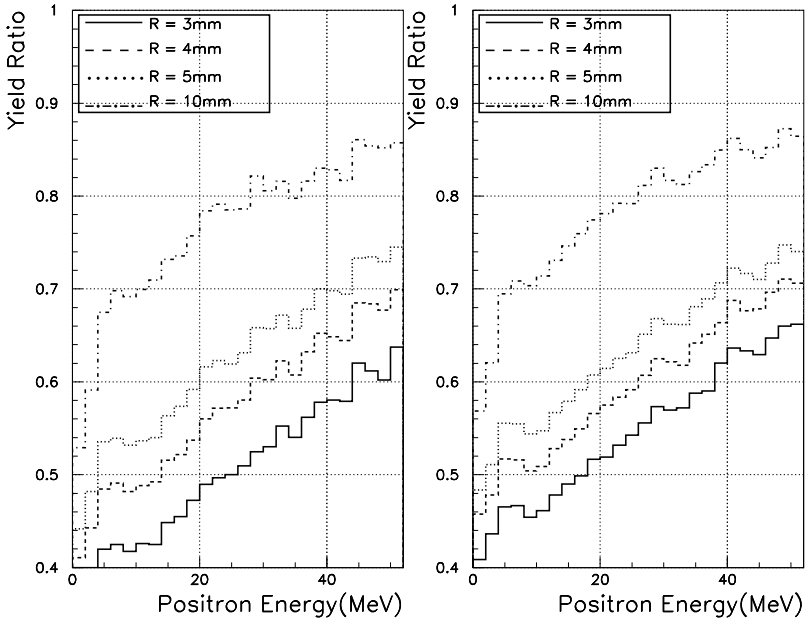

Figure 5: Ratio of positron yield per ΔE=2 MeV from the cone copper target (R_1=5 mm, R_2=3 mm) to that from the tungsten disc. a) E_{e^-}=3.11 GeV, σ_x=σ_y= 1.2 mm (left); b) E_{e^-}=6.22 GeV, σ_x=σ_y= 1.6 mm (right).

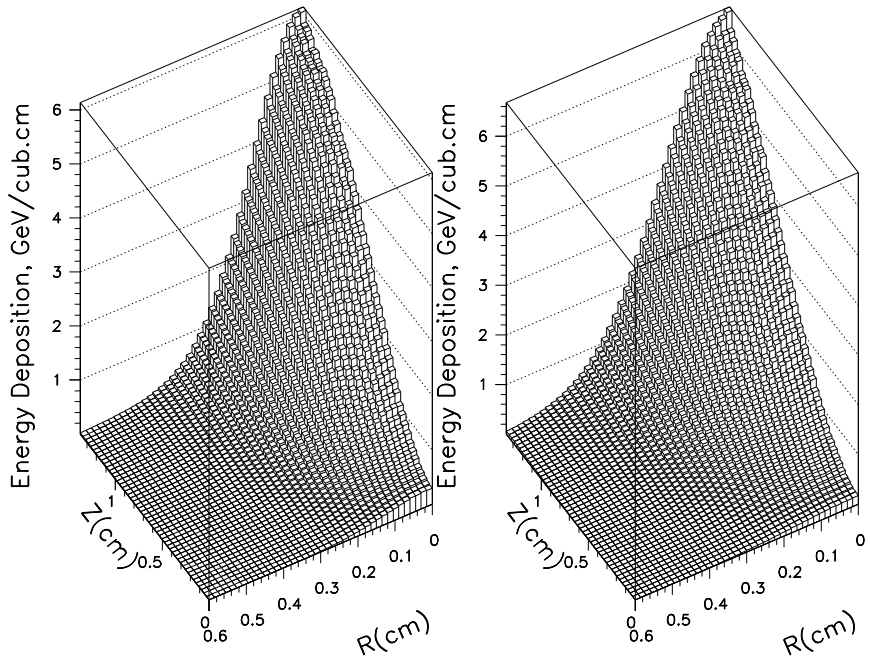

Figure 6: Energy deposition in a tungsten target (R=6 mm) for NLC-I and NLC-II: a) E_{e^-}=3.11 GeV, σ_x=σ_y= 1.2 mm (left); b) E_{e^-}=6.22 GeV, σ_x=σ_y= 1.6 mm (right).

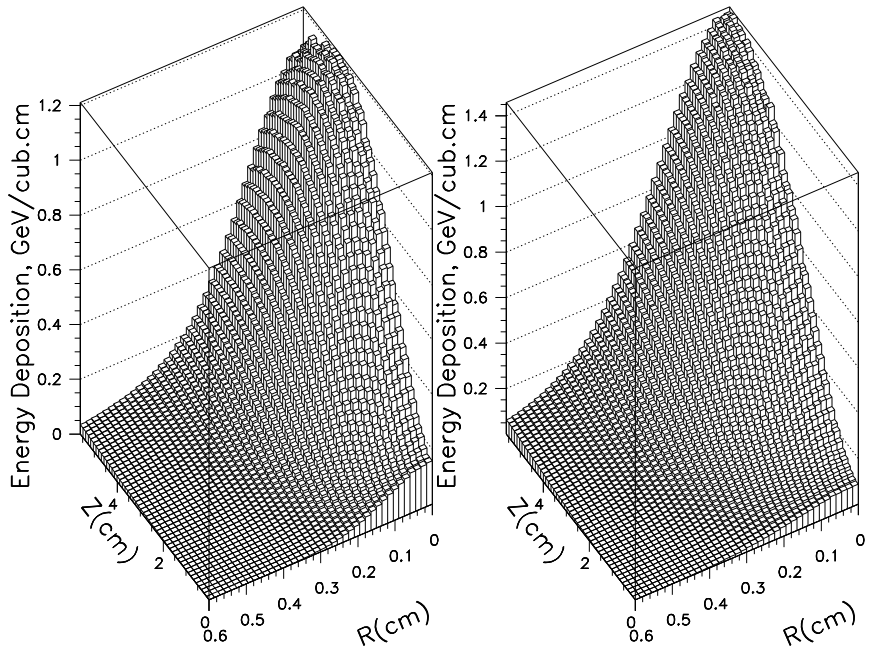

Figure 7: Energy deposition in a copper target (R=6 mm) for NLC-I and NLC-II: a) E_{e^-}=3.11 GeV, σ_x=σ_y= 1.2 mm (left); b) E_{e^-}=6.22 GeV, σ_x=σ_y= 1.6 mm (right).

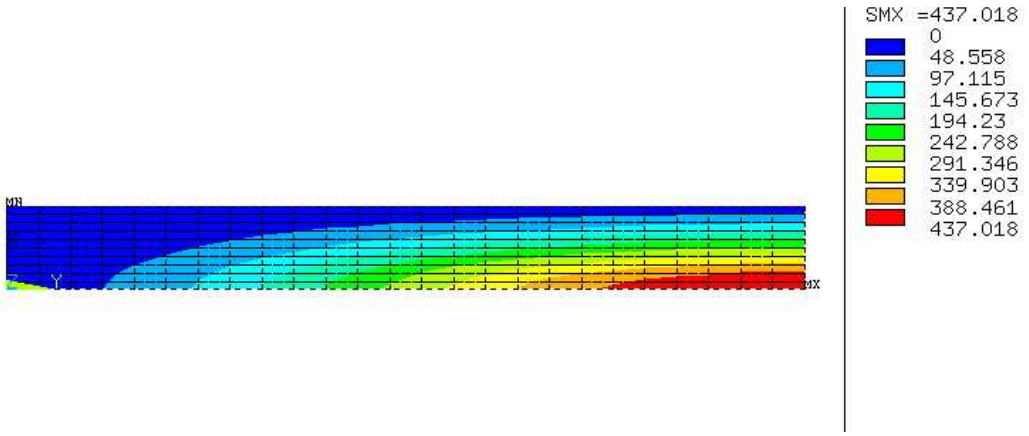

Figure 8: Temperature distribution after the pulse in a copper target (R=6 mm) for NLC-II. E_{e^-}=6.22 GeV, σ_x=σ_y= 1.6 mm.

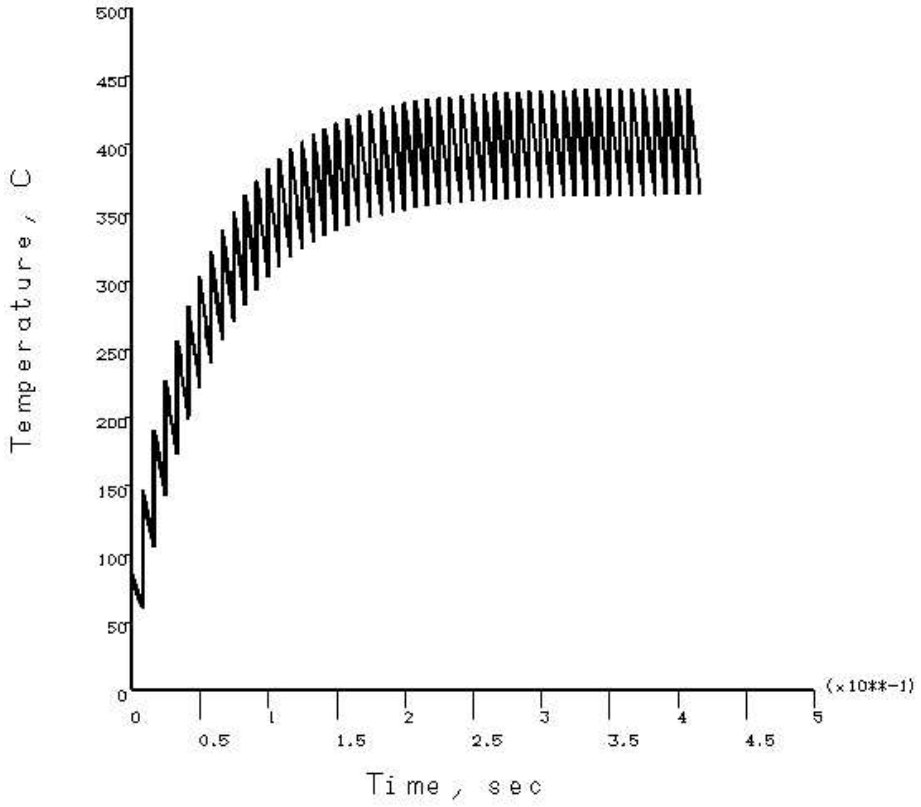

Figure 9: Time dependence of maximum temperature in a copper target (R=6 mm) for NLC-II. E_{e^-}=6.22 GeV, σ_x=σ_y= 1.6 mm.